ADVANCING EARTH AND SPACE SCIENCES

Geophysical Research Letters

RESEARCH LETTER
10.1029/2023GL106600

Key Points:

- Direct evidence of sunward transport of closed magnetic flux is observed by Magnetosphere Multiscale (MMS) at the dawn flank terminator
- MMS and Time History of Events and Macroscale Interactions during Substorms (THEMIS) observe nearly identical boundary layers at the dawn flank and pre-noon sectors
- Boundary layers and sunward convecting flux tubes are populated with energetic electrons and ring current oxygen ions

Correspondence to:
R. C. Rice,
rcrice@umd.edu

Citation:
Rice, R. C., Chen, L.-J., Gershman, D., Fuselier, S. A., Burkholder, B. L., Gurram, H., et al. (2024). Dynamics of the storm time magnetopause and magnetosheath boundary layers: An MMS-THEMIS conjunction. *Geophysical Research Letters*, *51*, e2023GL106600. https://doi.org/10.1029/2023GL106600

Received 2 OCT 2023
Accepted 30 JAN 2024

Dynamics of the Storm Time Magnetopause and Magnetosheath Boundary Layers: An MMS-THEMIS Conjunction

Rachel C. Rice[1,2], Li-Jen Chen[2], Dan Gershman[2], Stephen A. Fuselier[3,4], Brandon L. Burkholder[2,5], Harsha Gurram[1,2], Jason Beedle[2,6], Jason Shuster[7], Steven M. Petrinec[8], Craig Pollock[9], Ian Cohen[10], Christine Gabrielse[11], Philippe Escoubet[12], and James Burch[3]

[1]PHaSER, Department of Astronomy, University of Maryland, College Park, MD, USA, [2]NASA Goddard Space Flight Center, Greenbelt, MD, USA, [3]Southwest Research Institute, San Antonio, TX, USA, [4]University of Texas, San Antonio, TX, USA, [5]University of Maryland, College Park, MD, USA, [6]Catholic University of America, Washington, DC, USA, [7]University of New Hampshire, Durham, NH, USA, [8]Lockheed Martin Advanced Technology Center, Palo Alto, CA, USA, [9]Denali Scientific, LLC, Healy, AK, USA, [10]Applied Physics Laboratory, Johns Hopkins University, Baltimore, MD, USA, [11]Aerospace Corporation, El Segundo, CA, USA, [12]European Space Research and Technology Center, Noordwijk, the Netherlands

Abstract This letter uses simultaneous observations from Magnetosphere Multiscale (MMS) and Time History of Events and Macroscale Interactions during Substorms (THEMIS) to address the dynamics of the magnetopause and magnetosheath boundary layers during the main phase of a storm during which the interplanetary magnetic field (IMF) reverses from south to north. Near the dawn terminator, MMS observes two boundary layers comprising open and closed field lines and containing energetic electrons and ring current oxygen. Some closed field line regions exhibit sunward convection, presenting an avenue to replenish dayside magnetic flux lost during the storm. Meanwhile, THEMIS observes two boundary layers in the pre-noon sector which strongly resemble those observed at the flank by MMS. Observations from the three THEMIS spacecraft indicate the boundary layers are still evolving several hours after the IMF has turned northward. These observations advance our knowledge of the dynamic magnetopause and magnetosheath boundary layers under the combined effects of an ongoing storm and changing IMF.

Plain Language Summary Earth's magnetic field, the magnetosphere, acts as a shield protecting the near Earth environment from the solar wind. During active times, this shield can be damaged and reduced in size, but during quieter times, the shield can expand and repair itself. This letter uses observations from multiple spacecraft to better understand how the edges of our magnetosphere change during the transition from active to more quiet times. We observe the development of boundary layers at the dayside and flanks of the magnetosphere. Convection in and around these layers can contribute to the growth of the magnetosphere after it has been eroded during active times. These observations also place limits on the size of the boundary layers and how quickly they may develop.

1. Introduction

When the interplanetary magnetic field (IMF) is primarily pointed southward, as is often the case during geomagnetic storms, it reconnects with the Earth's northward field at the dayside magnetopause. The newly opened field lines offer a path for energized solar wind plasma to penetrate the magnetosphere. Dayside reconnection erodes the dayside magnetosphere as reconnected field lines move tailward.

Exactly where and how dayside flux is replenished during a storm remains an open question. Recent results show closed magnetic flux is reduced up to 35% on the dayside during the main phase of geomagnetic storms (Akhavan-Tafti et al., 2020). Convection processes in the tail related to storms are well described (Baumjohann, 2002; Yahnin et al., 1994), but processes for restoring the dayside closed flux are often overlooked. Magnetohydrodynamic (MHD) simulations by Hsieh and Otto (2014) show sunward convection away from the midnight sector as a significant contributor to flux depletion and the thinning of the tail current sheet, yet how far dayside this sunward convection can reach is not addressed. In situ observations of sunward convection away from the nightside plasma sheet contributing to the replenishment of closed dayside flux have not yet been reported.

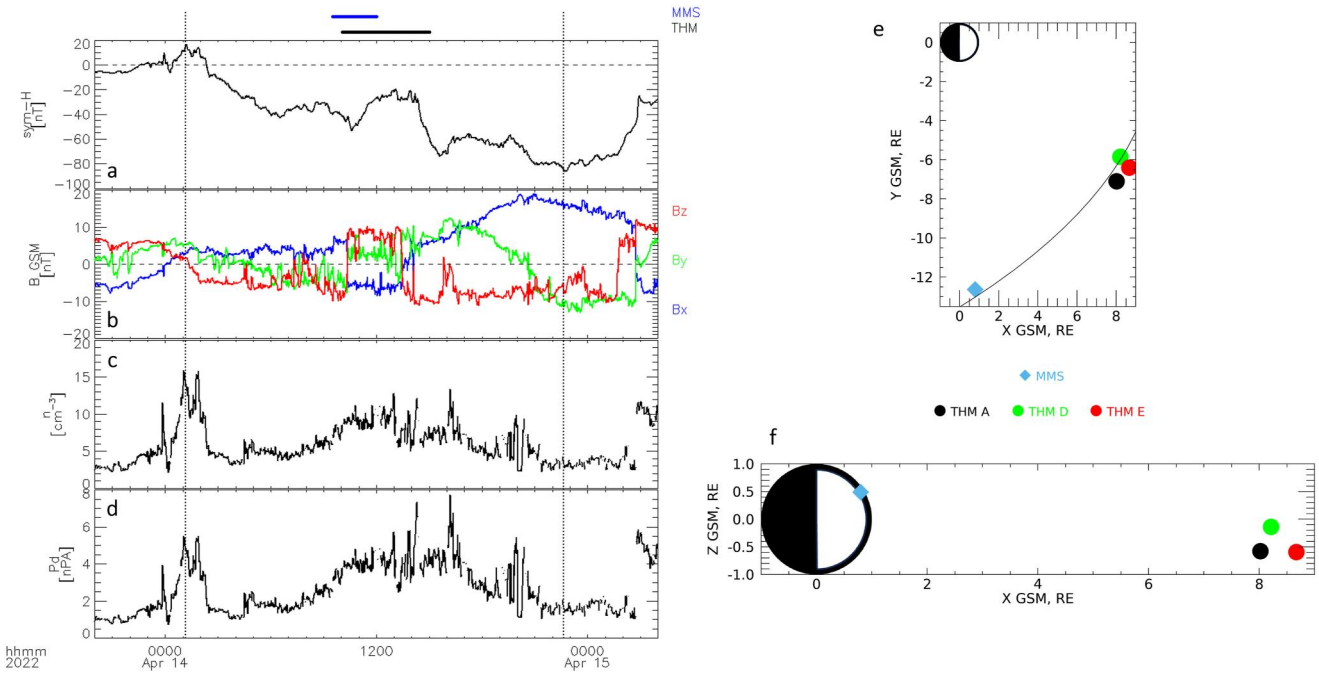

Figure 1. The storm on 14 April 2022 as seen in OMNI data: sym-H (a), interplanetary magnetic field (b), solar wind density (c), and dynamic pressure (d). The storm main phase lasted from 01:10 to 22:39 UT (vertical dotted lines). Magnetosphere multiscale (MMS) and Time History of Events and Macroscale Interactions during Substorms (THEMIS) observations of the dawn flank and pre-noon sectors (e, f) will be shown during intervals indicated by the blue and black bars, respectively (at top of panels a–d).

On the other hand, for primarily northward orientations of the IMF, dayside reconnection is expected to occur poleward of the cusps. The reconnected flux is thought to replenish the dayside magnetosphere and enable it to expand (Petrinec & Russell, 1993). The impact of IMF orientation is particularly noticeable in the low latitude boundary layer (LLBL), the region of mixed magnetosheath and magnetosphere plasma just inside the equatorial magnetopause. Observations have shown the LLBL is thicker when the IMF is northward (Lavraud et al., 2005; Li et al., 2005; Mitchell et al., 1987; Nakamura, 2021; Němeček et al., 2015; Øieroset et al., 2008). During extended periods of northward IMF, the LLBL has been observed to take the form of the cold dense plasma sheet within the magnetosphere (Nakamura, 2021; Øieroset et al., 2008).

In this work, we report observations of boundary layer (BL) formation and dynamics to address the dayside flux replenishment. The mechanisms driving dayside magnetosphere and BL growth operate across scales and regions. Observations spanning locations and scale sizes are required to understand magnetopause and BL behavior during changing IMF and storms. Measurements are from the Magnetosphere Multiscale (MMS) (Burch et al., 2016) and Time History of Events and Macroscale Interactions during Substorms (THEMIS) (Angelopoulos, 2008) missions during the main phase of a geomagnetic storm with a sudden IMF change.

2. Observations

On 14 April 2022, OMNI recorded a decrease in sym-H characteristic of a geomagnetic storm (Figure 1a). Storm loading begins around 00:00 UT with increases in solar wind density and pressure (Figures 1c and 1d) and a southward turning of the IMF (Figure 1b). The storm main phase begins at 01:10 UT on the fourteenth when sym-H peaks and ends at at 23:39 UT when sym-H reaches its minimum (Figure 1, dotted lines).

An IMF reversal occurs during the storm main phase. Between 10:20 and 10:22 UT all three components of the IMF make sudden and complete reversals, with B_Z turning from southward to northward (Figure 1b). This new orientation persists until 13:28 UT, when B_X and B_Z return to their initial values. Geotail, located approximately 8 R_E upstream of the bow shock, confirms the OMNI observations and timing. MMS and THEMIS

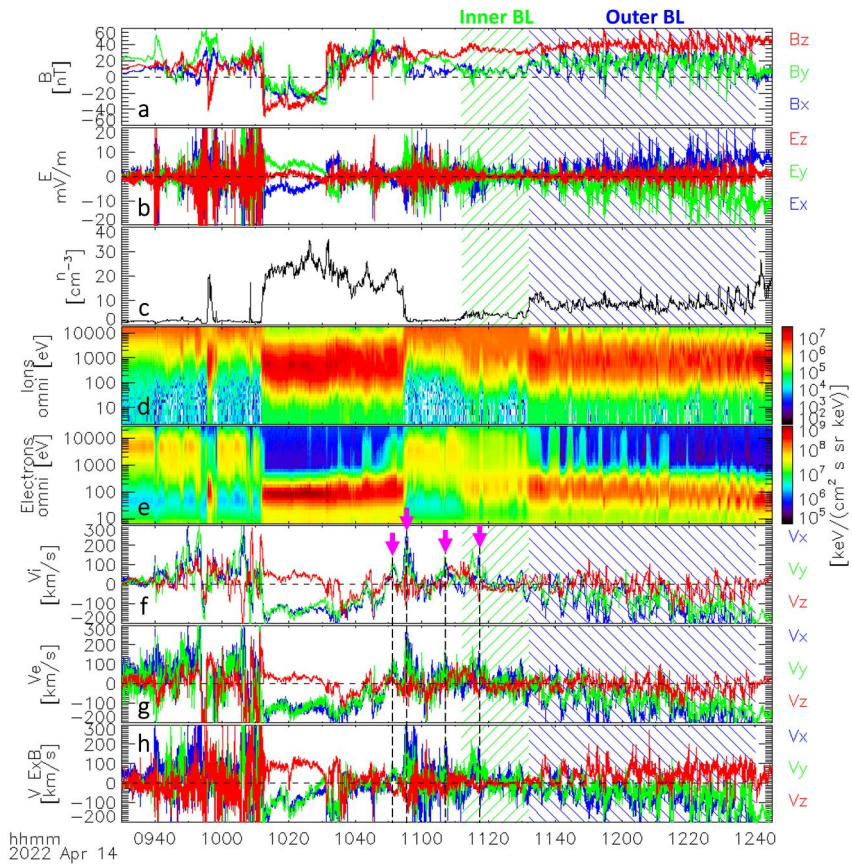

Figure 2. An overview of MMS1 measurements during magnetopause and boundary layer (blue, green hatching) encounters in the main phase of a geomagnetic storm when the interplanetary magnetic field reverses: geocentric solar magnetospheric magnetic field (a), electric field (b), density (c), ion (d) and electron (e) omnidirectional energy spectrograms, ion (f) and electron (g) bulk velocities, and $E \times B$ drift velocity (h). Sunward flows exceeding 100 km/s are marked with magnenta arrows, dashed lines.

capture the IMF turning and magnetospheric response from the equatorial dawn flank and pre-noon sectors, respectively (Figures 1g and 1h).

2.1. MMS

MMS observes strong sunward flows near the dawn flank magnetopause during northward IMF (Figures 2 and 3, magenta arrows). While MMS is embedded in sheath like plasma, it observes ion and electron velocities (Figures 2f and 2g) near 100 km/s in the sunward and duskward directions, directly opposite to the typical flow in the dawn flank sheath. MMS continues to observe brief periods of sunward flow exceeding 100 km/s as it enters the magnetosphere and encounters BLs. The sunward flows occur at times when E_Y is large and the magnetic field is dominated by northward B_Z, and thus match the local $E \times B$ drift velocity (Figure 2h).

Observations of energetic populations illuminate the magnetic connectivity in the regions of sunward flow (Figure 3). Electrons with energies from 70 to 100 keV (Figure 3e) show enhanced flux across all pitch angles, while higher energy electron flux (Figure 3f) is concentrated around 90° pitch angles, indicating closed field lines. The first and second regions of sunward flow (dashed lines, Figure 3) are separated by a region in which 70–100 keV energetic electron flux (Figure 3e) is strongest around 180° pitch angles, indicating the two regions are separated by open field lines and showing the dynamic 3D magnetopause with structures not seen during non-storm times. Reconnection closing flux tailward of MMS represents a possible driver for the replenishment of magnetospheric flux lost during the storm and for the growth of flank BLs.

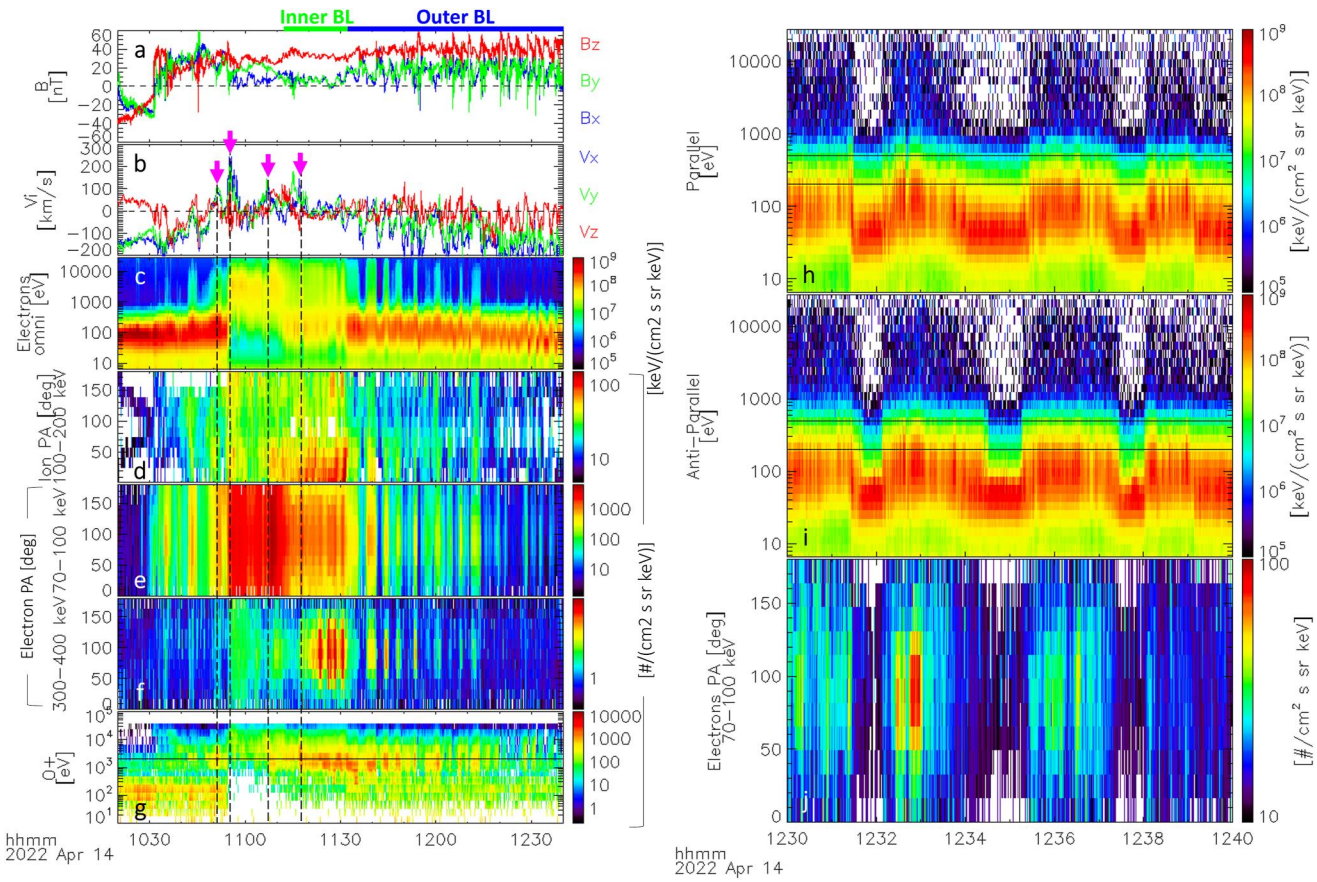

Figure 3. Sunward flows occur on closed field lines around the magnetopause observed by Magnetosphere Multiscale (MMS). Geocentric solar magnetospheric magnetic field (a), ion velocity (b), electron omnidirectional energy spectrogram (c), pitch angle distributions for 100–200 keV ions (d) and 70–100 keV (e), 300–400 keV electrons (f), and oxygen ion energy spectrogram (g). Sunward flows exceeding 100 km/s are marked with magenta arrows, dashed lines. A comparison of (h) parallel and (i) anti-parallel supra-thermal electrons are shown when the flux of 70–100 keV electrons (j) is low.

Oxygen ions consistent with ring current populations are present in the regions of sunward flow (Figure 3g). O+ flux above 2 keV (solid black line, data below 2 keV are mixed with instrumental effects from H+ and excluded from the interpretation) is enhanced at the closed field line regions with sunward flow (dashed lines).

Following the northward IMF turn, MMS observes magnetopause BLs which were not previously present. Significant flux enhancements of energetic electrons (Figure 3e) and O+ ions (Figure 3g) begin with the IMF turn, suggesting MMS is on field lines with at least one footprint in the ionosphere. At 10:55 UT, MMS re-encounters the magnetopause and remains in the magnetosphere until 11:12 UT. From 11:12 to 11:32 UT (Figure 2, green hatching) MMS observes increased density, about twice the magnetospheric value, and lower energy ions and electrons. From 11:32 to 12:40 UT (Figure 2, blue hatching), the density increases again, to about half the previously observed sheath density. Ion and electron spectrograms indicate the primary populations are at sheath energies with lower intensity than previously observed. Additionally, a variable high energy population appears in quasi-periodic bursts. The quasi-periodic high energy populations correspond with fluctuations in density, bipolar variations in the magnetic field component normal to the boundary, and decreases in total pressure consistent with Kelvin-Helmholtz (KH) waves.

The energetic populations further clarify the magnetic field line configuration of the observed BLs (Figure 3). In the inner BL from 11:12 to 11:32 UT (green bar at top), energetic (70–100, 300–400 keV) electrons are trapped on closed field lines (Figures 3e and 3f), with significant flux centered around 90° pitch angles. However, energetic ions (100–200 keV) in the region are mostly streaming parallel to the field, with intermittent anti-parallel streaming populations (Figure 3d). Energetic ions show some pitch angle dispersion, with lower pitch angle

ions arriving before those with higher pitch angles, suggesting a relatively fresh source for these energetic ions south of the MMS location. Ring current oxygen is also present within the inner BL (Figure 3g).

The magnetic configuration of the outer BL is mixed. From 11:32 to 12:40 UT (Figure 3, blue bar), energetic (70–100, 300–400 keV, Figures 3e and 3f) electrons appear on closed field lines quasi-periodically. O+ flux is also enhanced in these regions (Figure 3g). Where the flux of energetic electrons is small (e.g., 12:30–12:40 UT, Figure 3, right) we rely on the supra-thermal electrons between 200 and 500 eV to determine field line configuration (Fuselier et al., 2012, 2014). At 12:32, 12:35, and 12:38 UT supra-thermal electrons have larger flux in the parallel direction (Figure 3h) than the anti-parallel direction (Figure 3g), indicative of a field line with one footprint in the ionosphere south of MMS and the other open to the magnetosheath. Fluxes of parallel and anti-parallel supra-thermal electrons are more symmetric coinciding with closed field lines.

We note the first magnetopause crossing during northward IMF strongly resembles previous southward IMF crossings. Even though energetic electron and O+ populations are present immediately following the northward IMF turn, the plasma density and energy are unchanged from sheath-like values. The crossing around 10:55 UT is a sharp transition between the higher energy (Figures 2d and 2e), lower density (Figure 2c) plasma of the magnetosphere and the lower energy, higher density magnetosheath, with no intermediate energy or density indicative of a BL, much like the partial and full magnetopause crossings before 10:20 UT. Later crossings through the BLs are slower and contain intermediate plasma populations.

2.2. THEMIS

THEMIS encounters two BLs in the pre-noon sector after the IMF turns northward (Figure 4). The layers are still evolving hours after the IMF reversal and are at least thick enough to span the spacecraft separation.

All three THEMIS spacecraft encounter the first of two BLs (Figure 4, cyan bars above respective panels) less than an hour after the IMF's northward turn. Density in the outer layer is approximately one-half of the magnetosheath value (Figure 4b). Ion (Figures 4g–4i) and electron (Figures 4j–4l) energies are increased and variable. The magnetic field (Figures 4d–4f) and bulk velocity (Figure 4a) are also highly variable.

Immediately following the outer BL, THEMIS encounters a second unique layer (Figure 4, magenta bars). The density of the inner layer is about twice that of the magnetosphere proper (Figure 4b). Both ions and electrons comprise two distinct populations: one typical of the high energy magnetosphere and one with lower energy (Figures 4g–4l). Fluctuations in the magnetic field which persisted throughout the outer BL are not present in the inner layer (Figures 4d–4f).

We note both BLs are evolving at the time of observation and exhibit no evidence of plasmaspheric plumes. At the edge of outer layer, THEMIS D and A (Figures 4g and 4h) observe a small gap in the intense core population of ions, while THEMIS E (Figure 4i) observes a more extended decrease in the upper energy of the core ion population. Throughout the layer, THEMIS A and E observe more variable ion and electron energies and magnetic field than THEMIS D. The loss of intensity in the core ion population is more abrupt for THEMIS A and E than THEMIS D.

In the inner BL a strong band of electrons forms the core of the energy spectrograms for all three spacecraft. THEMIS D (Figure 4j) observes this band spanning energies from 100 to 500 eV, but for only a fraction of the layer. THEMIS A and E (Figures 4k and 4l) observe a thinner band, spanning energies from 300 to 500 eV, which persists for the entirety of the BL.

The pre-noon BLs are larger than typical. Previous missions have traversed dayside BLs in a few minutes (Fuselier et al., 2012, 2014; Lavraud et al., 2005). Each of the THEMIS spacecraft observe the layers for roughly 2 hr in the present case (Figure 4, cyan and magenta bars). The spacecraft separations place a lower bound on the dimensions of both BLs. From 11:21 to 11:39 and from 12:22 to 13:12 UT all three spacecraft are within the outer and inner BL, respectively. Maximum separations during those times are 0.62, 1.30, and 0.44 R_E and 0.75, 1.42, and 0.41 R_E in the geocentric solar magnetospheric -X, -Y, and -Z directions, respectively. In both cases the BLs must be at least large enough to span the spacecraft separation in all directions.

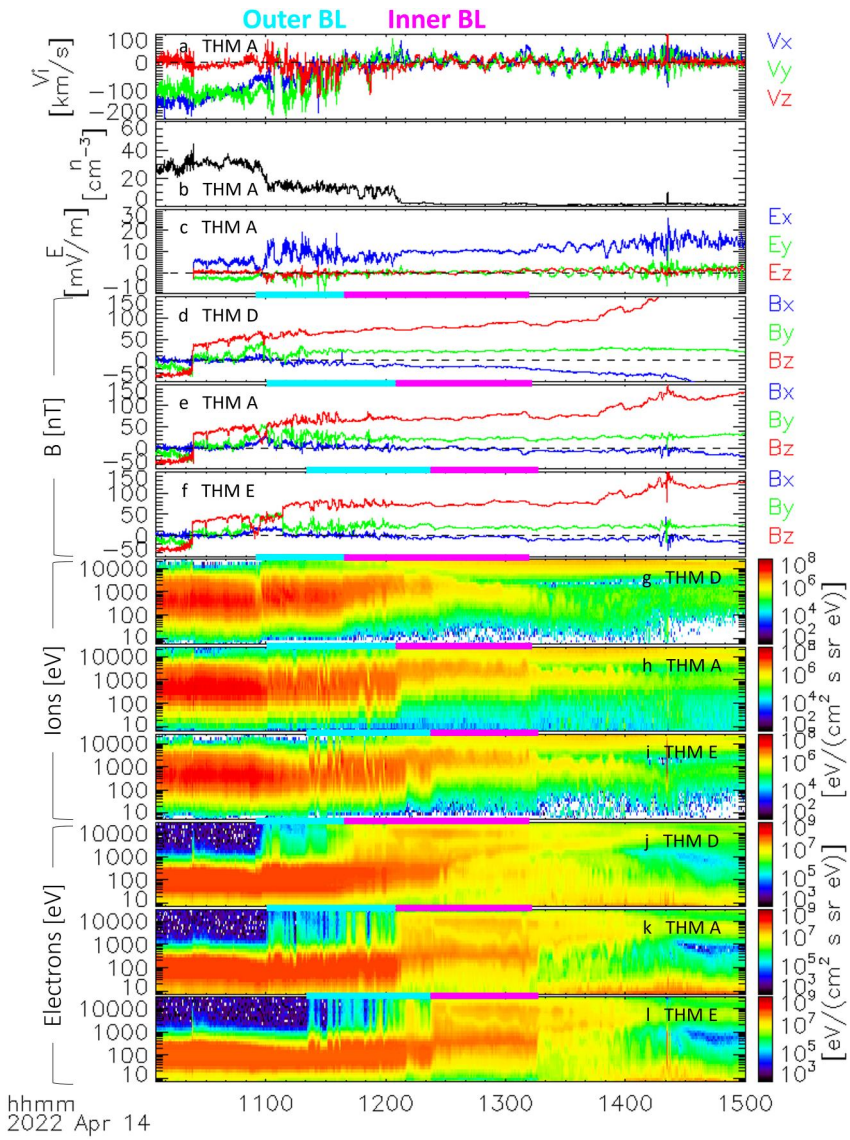

Figure 4. Time History of Events and Macroscale Interactions during Substorms (THEMIS) observations of the interplanetary magnetic field reversal and evolving BLs in the pre-noon sector: outer (cyan) and inner (magenta) BLs as seen in geocentric solar magnetospheric ion velocity (a), density (b) and electric field (c) by THEMIS A, and in magnetic field (d–f) and ion (g–i) and electron (j–l) omnidirectional energy spectrograms by THEMIS D, A, and E.

3. Comparing MMS and THEMIS BLs

Both MMS and THEMIS observe two BLs. Qualitative and quantitative similarities between MMS and THEMIS observations indicate they are observing the same BLs (Figure 5).

Strong similarities are evident in the outer BLs at MMS and THEMIS. MMS observes core populations similar to, but less intense than, those of the magnetosheath. A weaker and variable population extending to around 10 keV augments the core (Figures 2d and 2e). Likewise, THEMIS observes core populations similar to the sheath with a weaker, variable population extending above 10 keV (Figures 4g–4l). At both MMS and THEMIS the outer BLs' density (Figures 2c and 4b) is about half that of the adjacent magnetosheath and the magnetic field (Figures 2a and 4d–4f) is variable. The outer BLs at both observation locations comprise plasma of the same density and temperature (Figure 5) which is consistent with previous descriptions and observations of the magnetosheath boundary layer (MSBL) (Fuselier et al., 2012; Nakamura, 2021).

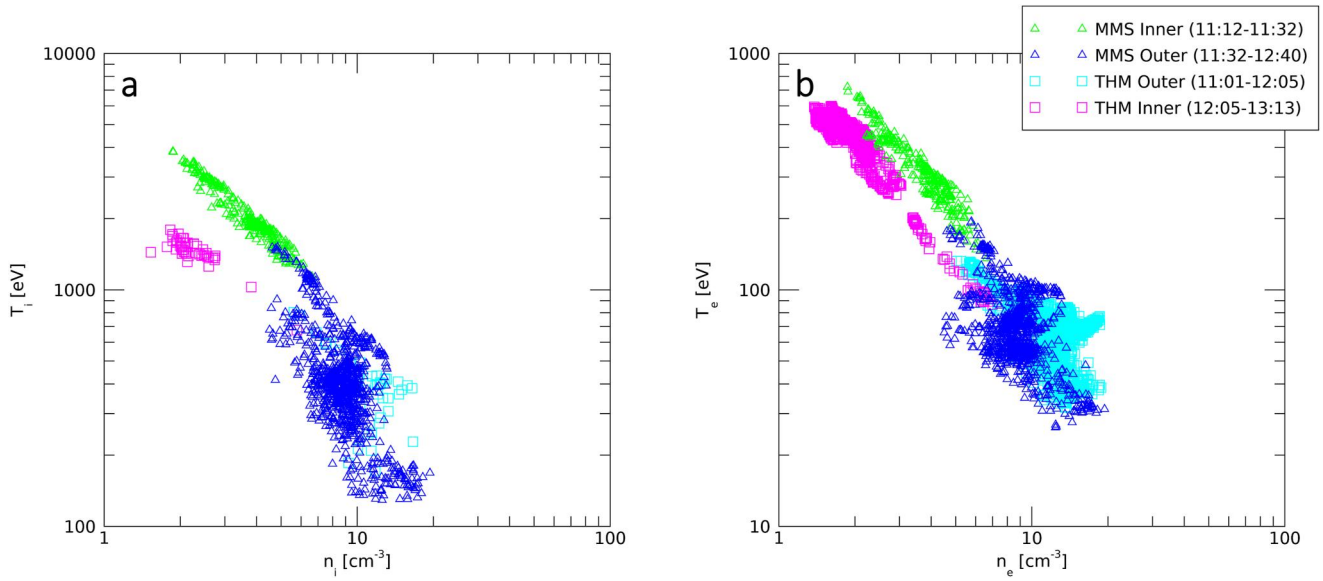

Figure 5. A comparison of ion (a) and electron (b) density and temperature in the BLs at Magnetosphere Multiscale (MMS) and Time History of Events and Macroscale Interactions during Substorms (THEMIS).

The density of the inner BLs at both MMS and THEMIS is about twice that of the magnetosphere (Figures 2c and 4b) and the magnetic field is relatively steady (Figures 2a and 4d–4f). The magnetosphere population is clearly present in both regions, and spectrograms show extensions to lower energies more typical of the magnetosheath (Figures 2d and 2e and 4g–4l). The inner BLs resemble previous descriptions and observations of the LLBL and cold dense plasma sheet (Nakamura, 2021; Øieroset et al., 2008).

The strong similarities in BL plasma at both the MMS and THEMIS locations may be a result of either a common generation mechanism or plasma transport. Several mechanisms are known contributors to the growth of the BLs: high latitude reconnection near the cusps, the KH instability, and kinetic Alfvén waves. KH waves are well developed at the dawn terminator, and may be in early stages of development in the pre-noon sector (e.g., the cyan interval in Figures 4e, 4f, 4h, 4i). Evidence of kinetic Alfvén waves is inconclusive in MMS observations, but increased perpendicular ion temperatures (not shown) in the pre-noon sector may be related to wave activity near THEMIS. Closed magnetic field lines in the inner BL suggest reconnection is involved in BL growth. The convecting closed flux tubes observed at the flank are likely a result of reconnection tailward of the spacecraft. The convection of these flux tubes sunward from the flank could help produce the flank BLs, but is unlikely to be solely responsible for the pre-noon BLs.

4. Summary and Discussion

The multi-mission observations reported here reveal a new picture of nightside reconnection driving dayside flux replenishment during stormtime and northward IMF. At the dawn flank, MMS observes the following key new features: (a) sunward convection of closed field lines around the magnetopause and (b) flux tubes populated with 70–100 keV electrons and O+ along with energized magnetosheath plasmas at approximately the time when IMF B_Z turns from southward to northward.

Our observations offer a new understanding of BL development during storm times. MMS and THEMIS observe two BLs with distinct plasma densities and temperatures in the dawn flank and pre-noon sectors 40 min after the northward IMF turn. Storm processes populate the BLs with energetic electrons and O+ ions which are not typical of quiet-time BLs. Energetic electrons and O+ ion populations are observed immediately following the IMF's northward turn, but plasma energy and density remain at sheath-like values, indicating that BL generation mechanisms start quickly but take tens of minutes to produce a BL with intermediate plasma energy and density.

Early observations of the LLBL by the International Sun-Earth Explorer (ISEE) satellites observed brief periods of sunward flow (Cowley, 1982; Sckopke et al., 1981), but the source and field line configuration of the ISEE observations could not be determined. In the current observations electron pitch angle distributions indicate regions of strong flow are located on closed field lines which convect sunward with the $E \times B$ velocity. Reconnection tailward of the spacecraft may produce the observed flux tubes. Preliminary MHD simulations indicate these flux tubes may originate at the tail reconnection site prior to the IMF's northward turning.

Storm processes likely populate the closed flux regions and BLs with 70–100 keV energetic electrons and ring current O+. Energetic electrons are observed at lower intensity within KH vortices, which is not typical of quiet-time KH observations in MMS data (Rice et al., 2022).

Two magnetopause BLs are observed simultaneously in the pre-noon and dawn flank sectors during a geomagnetic storm shortly after an IMF reversal from south to north. The outer BL comprises open and closed field lines. The inner BL contains only closed field lines, as expected for the LLBL. Both BLs are observed by multiple spacecraft in the pre-noon sector and near the dawn terminator. Multi-spacecraft observations further constrain the spatial extent and time scale of the BLs.

The observed inner BL is consistent with previous descriptions of the LLBL (Nakamura, 2021; Øieroset et al., 2008). Open field lines in the outer BL are indicative of the MSBL (Fuselier et al., 2012; Nakamura, 2021). Closed field lines in the outer BL may be related to high latitude reconnection, mixing within KH vortices, or KH induced double reconnection (see e.g. Eriksson et al., 2021; Ma et al., 2017).

The duration of the BLs in the pre-noon sector may be a result of the ongoing storm. Previous dayside BL observations typically last a few minutes (Fuselier et al., 2012, 2014; Lavraud et al., 2005). The BLs presented here persist for hours and are, at minimum, thick enough to span the spacecraft separation.

Data Availability Statement

MMS and THEMIS data are from the MMS Science Data Center (MMS [Dataset], 2022) and the Berkeley repository (THEMIS [Dataset], 2023), respectively. OMNI data are from NASA Goddard Space Flight Center's Space Physics Data Facility (Papitashvili & King, 2020).

Acknowledgments
This work is funded by the MMS mission, particulary through early career Grant 80NSSC23K1601. The authors thank the MMS and THEMIS teams and Vassilis Angelopoulos. Thanks also to Dr. Hasegawa and Dr. Nagai for their assistance with GEOTAIL data.

References

Akhavan-Tafti, M., Fontaine, D., Slavin, J. A., Contel, O. L., & Turner, D. (2020). Cross-scale quantification of storm-time dayside magnetospheric magnetic flux content. *Journal of Geophysical Research: Space Physics*, *125*(10). https://doi.org/10.1029/2020JA028027

Angelopoulos, V. (2008). The THEMIS mission. *Space Science Reviews*, *141*(1–4), 5–34. https://doi.org/10.1007/s11214-008-9336-1

Baumjohann, W. (2002). Modes of convection in the magnetotail. *Physics of Plasmas*, *9*(9), 3665–3667. https://doi.org/10.1063/1.1499116

Burch, J. L., Moore, T. E., Torbert, R. B., & Giles, B. L. (2016). Magnetospheric Multiscale overview and science objectives. *Space Science Reviews*, *199*(1–4), 5–21. https://doi.org/10.1007/s11214-015-0164-9

Cowley, S. W. H. (1982). The causes of convection in the Earth's magnetosphere: A review of developments during the IMS. *Reviews of Geophysics and Space Physics*, *20*(3), 531–565. https://doi.org/10.1029/RG020i003p00531

Eriksson, S., Ma, X., Burch, J. L., Otto, A., Elkington, S., & Delemere, P. A. (2021). MMS observations of double mid-latitude reconnection ion beams in the early non-linear phase of the Kelvin-Helmholtz instability. *Frontiers in Astronomy and Space Sciences*, *8*. https://doi.org/10.3389/fspas.2021.760885

Fuselier, S. A., Petrinec, S. M., Trattner, K. J., & Lavraud, B. (2014). Magnetic field topology for northward IMF reconnection: Ion observations. *Journal of Geophysical Research: Space Physics*, *119*(11), 9051–9071. https://doi.org/10.1002/2014JA020351

Fuselier, S. A., Trattner, K. J., Petrinec, S. M., & Lavraud, B. (2012). Dayside magnetic topology at the Earth's magnetopause for northward IMF. *Journal of Geophysical Research*, *117*(A8). https://doi.org/10.1029/2012JA017852

Hsieh, M.-S., & Otto, A. (2014). The influence of magnetic flux depletion on the magnetotail and auroral morphology during the substorm growth phase. *Journal of Geophysical Research: Space Physics*, *119*(5), 3430–3443. https://doi.org/10.1002/2013JA019459

Lavraud, B., Thomsen, M. F., Taylor, M. G. G. T., Wang, Y. L., Phan, T. D., Schwartz, S. J., et al. (2005). Characteristics of the magnetosheath electron boundary layer under northward interplanetary magnetic field: Implications for high-latitude reconnection. *Journal of Geophysical Research*, *110*(A6). https://doi.org/10.1029/2004JA010808

Li, W., Reader, J., Dorelli, J., Oieroset, M., & Phan, T. D. (2005). Plasma sheet formation during long period of northward IMF. *Geophysical Research Letters*, *32*(12). https://doi.org/10.1029/2004GL021524

Ma, X., Delamere, P., Otto, A., & Burkholder, B. L. (2017). Plasma transport driven by the three-dimensional Kelvin-Helmholtz instability. *Journal of Geophysical Research: Space Physics*, *122*(10). https://doi.org/10.1002/2017ja024394

Mitchell, D. G., Kutchko, F., Williams, D. J., Eastman, T. E., Frank, L. A., & Russell, C. T. (1987). An extended study of the low-latitude boundary layer on the dawn and dusk flanks of the magnetosphere. *Journal of Geophysical Research*, *92*(A7), 7394–7404. https://doi.org/10.1029/JA092iA07p07394

MMS [Dataset]. (2022). Retrieved from https://lasp.colorado.edu/mms/sdc/public/about/browse-wrapper/

Nakamura, T. K. M. (2021). The Earth's low-latitude boundary layer. In *Magnetospheres in the solar system* (pp. 177–191). American Geophysical Union (AGU). https://doi.org/10.1002/9781119815624.ch12

Němeček, Z., Šafránková, J., Kruparova, O., Přech, L., Jelínek, K., Dušík, Š., et al. (2015). Analysis of the temperature versus density plots and their relationship to the LLBL formation under southward and northward IMF orientations. *Journal of Geophysical Research: Space Physics*, *120*(5), 3475–3488. https://doi.org/10.1002/2014JA020308

Øieroset, M., Phan, T. D., Angelopoulos, V., Eastwood, J. P., McFadden, J., Larson, D., et al. (2008). THEMIS multi-spacecraft observations of magnetosheath plasma penetration deep into the dayside low-latitude magnetosphere for northward and strong B_y IMF. *Geophysical Research Letters*. https://doi.org/10.1029/2008GL033661

Papitashvili, N. E., & King, J. H. (2020). OMNI 1-min data [Dataset]. NASA Space Physics Data Facility. https://doi.org/10.48322/45bb-8792

Petrinec, S., & Russell, C. T. (1993). External and internal influences on the size of the dayside terrestrial magnetosphere. *Geophysical Research Letters*, *20*(5), 339–342. https://doi.org/10.1029/93GL00085

Rice, R. C., Nykyri, K., Ma, X., & Burkholder, B. L. (2022). Characteristics of Kelvin-Helmholtz wave as observed by the MMS from September 2015 to March 2020. *Journal of Geophysical Research: Space Physics*, *127*(3). https://doi.org/10.1029/2021JA029685

Sckopke, N., Paschmann, G., Haerendel, G., Sonnerup, B. U. Ö., Bame, S. J., Forbes, T. G., et al. (1981). Structure of the low-latitude boundary layer. *Journal of Geophysical Research*, *86*(A4), 2099–2110. https://doi.org/10.1029/JA086iA04p02099

THEMIS [Dataset]. (2023). Retrieved from http://themis.ssl.berkeley.edu/data/themis/

Yahnin, A., Malkov, M. V., Sergeev, V. A., Pellinen, R. J., Aulamo, O., Vennerström, S., et al. (1994). Feature of steady magnetospheric convection. *Journal of Geophysical Research*, *99*(A3), 4039–4051. https://doi.org/10.1029/93JA02868

Yahnin, A., Malkov, M. V., Sergeev, V. A., Pellinen, R. J., Aulamo, O., Vennerström, S., et al. (1996). Feature of steady magnetospheric convection. *Journal of Geophysical Research*, https://doi.org/10.1029/93JA02868